

Evaluation of Smart Glazing Properties for Net Positive Windows in Commercial Buildings

Eric Ohene¹, Michael D. McGehee², Moncef Krarti¹

¹Department of Civil, Environmental and Architectural Engineering

²Department of Chemical Engineering
University of Colorado Boulder, USA

Abstract

The study identifies smart glazing properties necessary for delivering net energy positive performance for office buildings. A comprehensive parametric framework is used to quantify the influence of smart window optical and thermal characteristics, tint control strategies, and building design parameters on whole-building energy performance. The analysis results demonstrate that smart glazed windows can transition from net energy liability to net energy positive elements of office building envelopes when climate-responsive control strategies and daylighting integration are appropriately implemented. Without daylighting control, smart glazed windows can increase annual energy use by up to 20% in cooling-dominated climates, whereas the deployment of daylighting control reduced total energy consumption by 5-7% in mixed climates such as Boulder, CO. Outdoor air temperature (OAT)-based control strategies consistently outperformed incident total solar-radiation (ITSR)-based controls, when coupled with optimal switching settings. Moreover, the sensitivity analyses reveal a nonlinear dependence of energy performance on window-to-wall ratio, with large windows increasing both the penalties and benefits of smart glazed fenestration systems. Improvements in thermal transmittance below $1.10 \text{ W/m}^2 \cdot \text{K}$ yielded diminishing returns, indicating that adaptive optical properties are more influential than ultra-low U-factors for achieving net energy positive performance for smart glazed windows. The evaluation of commercially available electrochromic glazing products when deployed to office buildings show energy savings of 2–5% for mild and mixed climates, near-neutral performance for cooling-dominated climates, and energy penalties for heating-dominated climates.

Keywords: Net positive energy, office buildings, optical properties, optimal controls, smart glazing, windows.

Nomenclature

Abbreviations	
AL	Air Leakage
DOE	US Department of Energy
EMS	Energy Management System
HVAC	Heating, Ventilating, and Air Conditioning
IGU	Insulated Glass Unit
ITSR	Incident total solar radiation
NPW	Net positive window
OAT	Outdoor air temperature
SHGC	Solar heat gain coefficient
VT	Visible transmittance
WWR	Window-to-wall ratio

1. Introduction

Buildings account for 40% of the total US energy consumption. Over one-third of the US primary energy use of buildings are attributed to commercial spaces [1],[2], with heating, ventilation, and air conditioning (HVAC) systems are responsible for over 40% of this energy demand, largely due to thermal loads associated with heat losses and gains through the building envelope systems [3],[4]. Indeed, building envelopes have a critical role in energy efficiency, thermal comfort, and indoor environmental quality of buildings as they affect their heating, cooling, ventilation, and lighting demands [5]. Among envelope systems components, windows are often thermally the weakest component and can be responsible for up to 60% of total building energy demands due to their high thermal transmittance compared to opaque envelope elements [6]. Despite this inherent weakness, windows also present unique opportunities for reducing energy needs of buildings by facilitating daylight penetration and enabling beneficial solar heat gains when properly designed and controlled.

Recent advances in smart glazing technologies have transformed windows from passive envelope elements into adaptive systems capable of dynamically regulating solar, heat, and visible light transmissions. Unlike conventional static glazed fenestration systems and manually operated shading devices, smart glazed windows can modulate their optical properties in response to environmental conditions or control inputs, thereby reducing cooling loads during warm periods while maintaining daylight availability and beneficial solar gains during colder seasons [7]. In the US, the existing window stock is estimated to account for approximately 10% of total building

energy consumption. However, modeling studies suggest that this contribution could be reduced by up to 50% through the widespread deployment of smart window technologies [8],[9].

Based on their tint switching mechanisms, smart glazing systems may be classified into passive and active technologies. The passive smart glazing technologies, such as thermochromic (TC) and photochromic glazing, respond autonomously to changes in temperature or solar irradiance without external energy input. Active systems, including electrochromic (EC), gasochromic, suspended particle devices, and liquid crystal technologies, rely on externally applied electrical or chemical stimuli to change their optical properties [7],[10]. Previous modeling and experimental studies have reported that such systems can reduce annual heating and cooling energy use by up to 20–30% and achieve whole-building energy savings exceeding 40% under favorable conditions for commercial buildings [11], [12], [13], [14]. While the energy-saving capabilities of smart glazing are well documented, the majority of studies have focus on operational energy reductions, with limited attention given to the potential for their net positive performance when deployed to buildings. A net positive window (NPW) is defined as a fenestration system whose annual energy gains offset or exceed its associated energy losses, effectively transforming the window from a liability into a net contributor to building energy performance [15].

Although most installed fenestration systems still rely on conventional static windows with low-emissivity coatings [16], the adoption of smart glazing technologies has increased steadily over the past decade. Advances in materials, controls, and manufacturing have improved the performance reliability and commercial viability of both passive and active smart glazing systems, contributing to their growing adoption [17]. This trend is reflected in market projections, which estimate that the global smart glass market will expand from USD 7.38 billion in 2024 to USD 13.01 billion by 2030, corresponding to a compound annual growth rate of 9.6% between 2025 and 2030 [18]. However, the rate of adoption of smart glazing depends on the outcomes of unbiased evaluations aimed at quantifying their energy and performance impacts.

Recent reviews have synthesized the state of advanced window technologies, with particular emphasis on electrochromic and other dynamically switchable glazings [19],[20],[21]. Complementary modeling and experimental studies have demonstrated the potential of smart fenestration systems to reduce building energy use across a wide range of climates and building types [22]. However, while these studies establish the energy-saving capability of smart glazing,

they generally do not assess whether such systems can be configured to offset their own energy losses and enhance the energy performance of buildings.

Prior research has examined the energy and comfort impacts of smart glazed fenestration systems under well-defined design and control strategies, consistently showing that performance outcomes are highly sensitive to climate, façade orientation, glazing properties, and daylight-responsive lighting controls [23],[24],[25],[26]. Smart glazing systems have been reported to achieve year-round energy savings of up to 11.2% relative to conventional double-glazed windows depending on their orientation [27] as well as to lower annual solar gains through fenestration systems by approximately 30% compared with fixed shading devices specially in hot and arid climates [28]. Additional studies have reported lighting energy savings ranging from 37% to 48% from the deployment of dynamic glazing systems instead static windows with occupant-operated blinds [29]. Optimized smart fenestration configurations have been shown to deliver whole-building energy savings exceeding 40% for U.S. office buildings [22], while switchable glazing with variable solar reflectance has demonstrated heating and cooling energy reductions of up to 23% when applied to medium-sized office buildings [11].

At the market and regional scales, the potential impact of smart glazing can be significant. Analyses of the U.S. building stock suggest that highly insulating smart windows could reduce annual energy consumption in residential and commercial buildings by approximately 4.5% [30]. Other studies further indicate HVAC energy reductions exceeding 17% for office buildings across multiple cities in China [31], with reported savings of up to 28% and 11% for Shanghai when compared with single clear and conventional double-pane glazing, respectively. Lifecycle assessments have also highlighted long-term benefits, with electrochromic windows achieving up to 54% cumulative energy reduction over a 25-year period in Greek office buildings relative to single-pane glazing systems [32]. These findings underscore the importance of dynamic solar and daylight control in mitigating peak cooling loads, reducing glare, and enhancing lighting energy savings.

Despite the reported energy-saving benefits, the practical performance of smart glazing remains limited by the optical and thermal properties of products currently available on the market. Table 1 presents typical ranges of key performance parameters for widely used smart window technologies. Electrochromic (EC) glazing demonstrates a broad tint modulation capability, with SHGC values varying from approximately 0.63 to 0.27 for the clear state and from 0.31 to as low

as 0.04 for the tinted state. Corresponding visible transmittance ranges from about 0.75 to 0.35 for the clear condition and from 0.17 to 0.01 for dark state, while reported U-factors span roughly 0.5 to 1.87 W/m²·K. Thermochromic (TC) glazing exhibits a narrower but still significant tint modulation range, with SHGC values decreasing from approximately 0.62–0.20 for the clear state to 0.45–0.10 for the dark state, and visible transmittance ranging from 0.60–0.26 and 0.13–0.04, respectively. The thermal performance of TC systems is characterized by U-factors between 1.31 and 2.76 W/m²·K. By comparison, photochromic (PC) glazing typically provides limited control over solar and visible transmissions and is associated with substantially higher thermal transmittance levels, with U-factors on the order of 5.7–5.9 W/m²·K.

Although dynamic optical properties allow window systems to respond to seasonal variations in solar radiation and daylight availabilities, there is still insufficient guidelines on how existing smart glazing products should be configured to deliver net energy benefits for commercial building applications. Indeed, existing studies that have explored net energy performance of advanced windows have focused predominantly on residential applications. For example, Apte and Arasteh [33] reported modest annual energy savings for dynamic windows in climates dominated by a single season, with improved performance observed in mixed climates. Similarly, Arasteh et al. [15] demonstrated that dynamic windows with relatively high maximum SHGC values could approach zero-energy behavior in northern residential climates without requiring ultra-low U-factors. However, these findings cannot be directly generalized to office buildings, which are characterized by higher internal loads, different occupancy patterns, and stronger interactions between glazing performance and daylight-responsive lighting systems. Moreover, prior work has not systematically evaluated the combined influence of optical switching thresholds, control strategies, daylighting integration, and building design parameters on the net energy balance of smart glazing fenestration systems when deployed to office buildings. Although a recent study examined net positive energy windows for office applications, its scope was limited to static glazing configurations [34]. Consequently, design-oriented guidance identifying the optical and thermal performance targets required for smart glazing systems to be net positive energy components of office building envelopes is still lacking.

To overcome the noted gap, this study develops a comprehensive parametric evaluation framework to examine the conditions under which smart glazed fenestration systems can achieve net-positive energy performance in office buildings. Using DOE commercial prototype buildings

both idealized parametric glazing configurations and commercially available smart glazing products are evaluated considering practical design and manufacturing constraints. The primary contributions of this work are threefold. First, the study assesses and compares outdoor air temperature-based and solar radiation-based switching control strategies for smart glazing. Second, the study identifies climate-specific ranges of clear-state and dark-state solar heat gain coefficients and visible transmittance values that enable smart glazing to transition from an energy liability to a net-positive energy performance. Third, commercially available smart glazing systems were evaluated to assess their energy performance across various U.S. climate zones, window sizes, and switching control strategies in office building applications. The findings reported in this work aim to inform future improvements in smart glazing product design and to offer actionable guidelines for building designers and engineers seeking to enhance whole-building energy performance through informed selection of fenestration systems.

Table 1. Thermal and optical properties for selected commercially available smart glazing products [35].

Manufacturer	Product	U-factor (W/m ² -K)	SHGC	VT
Electrochromic Windows				
SAGE	Double Glass SAGEGLASS BLUE	1.65	0.30–0.10	0.40–0.01
Electrochromics	Double Glass SAGEGLASS GRAY	1.65	0.33–0.10	0.45–0.01
	Double Glass SAGEGLASS GREEN	1.65	0.27–0.10	0.49–0.01
	Classic™ Tempered	1.59	0.47–0.09	0.62–0.02
	Double Glass See Green™	1.59	0.44–0.09	0.48–0.028
	Double Glass Cool View Blue™	1.59	0.46–0.09	0.40–0.023
	Double Glass Clear-as-Day™	1.59	0.46–0.09	0.35–0.019
	Double Glass SAGEGLASS CLEAR	1.59	0.41–0.09	0.60–0.01
	Classic™ Triple Glass Ar	1.25	0.42–0.07	0.55–0.01
EControl-Glas GmbH & Co.	Double Glass EControl smart®	1.1	0.38–0.10	0.50–0.10
	Smart Double Glass EControl®	1.1	0.42–0.10	0.56–0.10
	Double Glass EControl®	1.1	0.40–0.12	0.55–0.15
	Triple Glass EControl®	0.5	0.33–0.09	0.48–0.13
	Triple Glass EControl Smart®	0.5	0.33–0.08	0.45–0.09
	Smart Triple Glass EControl®	0.5	0.36–0.08	0.51–0.09
VIEW Inc.,	Double Glass Dual IGU High Altitude*	1.87	0.46–0.11	0.58–0.03
	Standard Dual Pane IGU	1.65	0.46–0.09	0.58–0.03
	Double Glass Dual IGU with Blue Tint	1.65	0.43–0.09	0.36–0.02
	Double Glass Dual IGU with Gray Tint	1.65	0.44–0.09	0.42–0.02
	Double Glass Dual Lami IGU	1.65	0.46–0.09	0.58–0.03
	Double Glass Dual IGU w/LowE on #3	1.36	0.33–0.07	0.49–0.03
	Double Glass Dual IGU w/LowE on #4	1.31	0.43–0.08	0.57–0.03

	Triple Glass Dual IGU with LowE	1.2	0.44–0.06	0.58–0.03
	Triple Glass Triple IGU	1.19	0.41–0.07	0.52–0.03
	Single Glass Conver Light™	5.5	0.63–0.31	0.66–0.17
	Double Glass Conver Light™	1.1	0.43–0.13	0.59–0.15
	Triple Glass Conver Light™	0.6	0.36–0.10	0.54–0.14
Thermochromic Window				
Pleotint LLC	Suntuitive with Solarban®70XL + Solargray	1.31	0.20–0.11	0.27–0.06
	Suntuitive with Solarban®70XL + Optiblue	1.31	0.26–0.12	0.39–0.08
	Suntuitive with Solarban®70XL + Azuria	1.31	0.24–0.11	0.42–0.09
	Suntuitive with Solarban® + Solarbronze	1.31	0.22–0.11	0.33–0.07
	Suntuitive with Solarban® 60 + Azuria	1.36	0.26–0.12	0.46–0.10
	Suntuitive with Solarban® 60 + Clear	1.36	0.37–0.17	0.60–0.13
	Suntuitive with Solarban® 60 + Solarblue	1.36	0.27–0.14	0.38–0.08
	Suntuitive with Solarban® 60 + Optiblue	1.36	0.31–0.16	0.43–0.09
RavenBrick, LLC	1-inch IGU (Standard lowE)	1.99	0.576–0.449	0.34–0.05
	1-inch IGU (Double Silver lowE)	1.63	0.221–0.108	0.29–0.04
	1-inch IGU (Clear Dual Pane)	2.76	0.620–0.499	0.37–0.06
Preleo	Prel-Shade (green tinted and Loe ² 272)	1.36	0.37–0.16	0.53–0.08
	Prel-Shade (Loe ³ 366)	1.31	0.23–0.10	0.48–0.07
Photochromic window				
Chameleon	Chameleon 10	-	0.31–0.22	0.13–0.10
	Chameleon 30	-	0.32–0.25	0.33–0.30
	Chameleon 50	-	0.36–0.34	0.52–0.42
Tint Station Window	Illume 20	-	0.31–0.22	0.16–0.09
Films PTE LTD	Illume 40	-	0.36–0.28	0.37–0.30
	Illume 60	-	0.42–0.36	0.56–0.47
	Illume 70R	-	0.43–0.37	0.69–0.57

2. Research method

Fig. 1 illustrates the analytical workflow adopted in this study to evaluate the energy performance impacts associated with the application of smart fenestration systems for office buildings. The assessment is based on the U.S. Department of Energy (DOE) medium office prototype model, which provides a consistent and widely accepted reference for evaluating building technologies, including alternative window systems and associated control strategies [36]. Annual building energy use is estimated using EnergyPlus, a dynamic whole-building performance engine capable of accurately predicting dynamic variations in thermal loads, solar gains, and daylight availabilities [37]. Smart glazing behavior is modeled using the Energy Management System (EMS) utility within EnergyPlus, which provides the flexibility to implement custom rule-based controls. This capability enabled systematic testing of control variables governing glazing state transitions.

This study adopts a three-step analysis approach. In the first step, a selection of market-ready smart glazing systems is evaluated to quantify their reference performance in a representative cool-dry climate of Boulder, CO, considering cases with and without daylighting control. The second step involves a comprehensive parametric assessment of key glazing attributes, systematically varying thermal and optical parameters to reveal performance patterns over a broad spectrum of SHGC and visible transmittance levels. For the final step, a series of sensitivity analyses is performed to determine the effects of climate, façade orientation, building scale, and window-to-wall ratio on the ability of smart glazing systems to support net positive energy performance for office buildings.

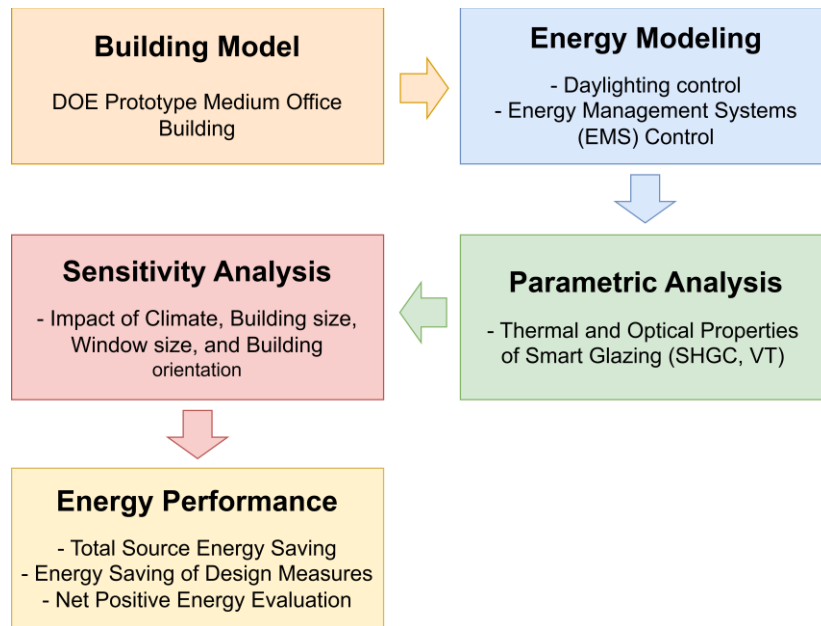


Fig. 1. Analysis approach framework adopted for this study.

2.2. Description of building energy model

The analysis is performed using DOE’s prototypical medium-sized office model, configured to comply with ASHRAE Standard 90.1-2019 requirements for new commercial buildings [36]. This prototype provides a complete and consistent representation of a contemporary office building, including envelope constructions, HVAC systems, lighting power densities, occupancy schedules, and miscellaneous equipment loads. The building features three identical stories, with each floor

divided into a central core zone and four surrounding perimeter zones, as illustrated in Fig. 2. The conditioned floor area totals 4,982 m² (53,628 ft²), and the façade incorporates a uniform window-to-wall ratio of 33% on all orientations. Space conditioning is delivered through a variable-air-volume (VAV) system with gas heating and packaged cooling units. Table 2 summarizes the key attributes of the prototype office building used in the simulations. This standardized configuration ensures that performance comparisons across climates and glazing scenarios are made without interference from unrelated variations in building envelope or mechanical systems.

Table 2. Summary of key characteristics of the simulated reference office building.

Variable	Description (value/unit)
Gross floor area	4,982 m ² (53,628 ft ²)
Aspect ratio	1.5
Thermal zoning	3 floors, 4 perimeter zones, 4.572 m (15 ft) depth around a central core zone; 40% perimeter space and 60% is core zone
Floor height	Floor-to-floor height of 3.96 m (13 ft), ceiling height 2.74 m (9 ft) and a 1.22 m (4 ft) plenum above
Wall construction	Steel-framed exterior wall with gypsum and stucco board, R-13.45 insulation layer
Roof construction	Metal-surfaced assembly R-20.83, emissivity of 0.9 and solar absorptance of 0.7
WWR	33%
Infiltration rate	0.5905 cfm/ft ² (3.0 L/s·m ²) at 0.30 in. water column
HVAC system	VAV system with packaged air-conditioning and gas-fired heating. Air-cooled chiller, dry-bulb temperature economizer. 80% thermal efficiency domestic hot water system
Thermostat setpoints	24 °C (75 °F) cooling setpoint 21 °C (70 °F) heating setpoint
Thermostat setbacks	Cooling setback of 27 °C (80 °F) Heating setback of 16 °C (60 °F)

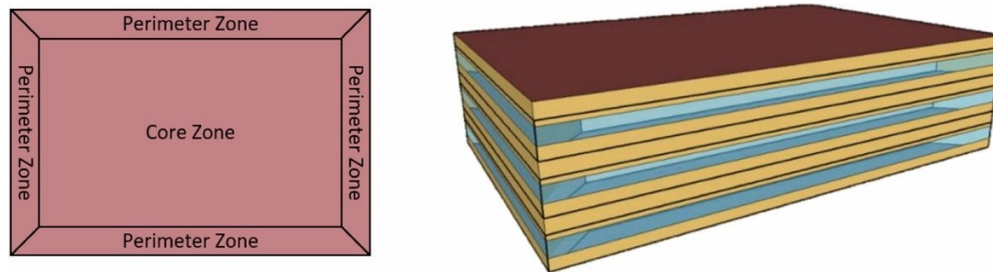


Fig. 2. DOE medium office building model [38].

2.3. Baseline energy model

To define a benchmark for evaluating alternative glazing configurations, the reference building model employs adiabatic, opaque, and completely air-sealed window surfaces. Under this assumption, the fenestration contributes no heat transfer, solar gains, or daylight effects, corresponding to $U\text{-factor} = \text{SHGC} = \text{VT} = \text{AL} = 0$. While such a configuration is not physically representative of a real window system, adiabatic window reference establishes a consistent analytical benchmark that facilitates systematic and unbiased comparison of glazing technologies, design configurations, and control strategies within the prototypical office building framework consistent with previous studies [15], [34], [39]. Fig. 3 illustrates the distribution of annual source energy use for the reference office building in Boulder, Colorado. The analysis indicate a total source energy use intensity of 246.88 kWh/m². Plug and miscellaneous equipment loads represent the largest share of the building end uses of 43%, with interior lighting accounting for 17%, space heating of 16%, domestic hot water of 8%, and cooling load of 7%. These end-use distributions reflect the building energy needs in the absence of fenestration-related heat transfer and daylight effects.

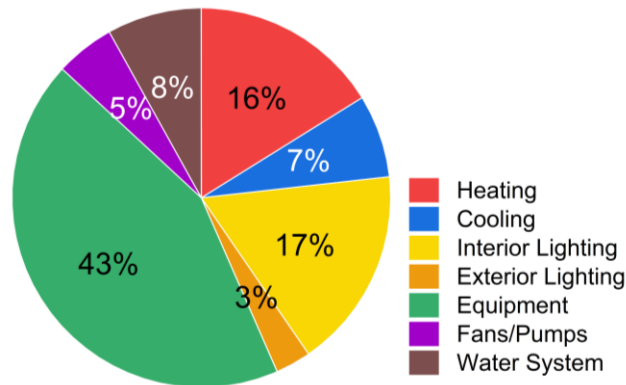


Fig. 3. Annual source energy end-use distribution for the baseline reference office building in Boulder, CO.

2.4. Smart Glazing Properties

The first stage of the analysis evaluated a set of commercially available smart glazing products applied to the medium office prototype. Table 3 presents the associated thermal transmittance (U -factor) and optical characteristics, namely the SHGC and VT, for both the clear and tinted states

of the four selected smart glazing systems. Two environmental variables are used to control glazing state transitions: outdoor air temperature (OAT) and incident total solar radiation (ITSR). These metrics collectively capture the primary drivers of solar heat gains and cooling loads in perimeter zones. Rule set based control algorithms are implemented using the Energy Management System framework in EnergyPlus to represent the switching behavior of commercially available smart glazing products. The control logic is formulated as a set of deterministic rules that govern transitions between clear and dark states in response to environmental and operational conditions, such as incident solar radiation and temperature-based control. At each simulation timestep, EMS sensors monitor relevant variables, and EMS actuators override the glazing state accordingly. This approach enables smart glazing to respond dynamically to changing outdoor and indoor conditions while maintaining stable and realistic switching patterns that are consistent with glazing specifications. By embedding the control logic within the EMS framework, the model captures the temporal behavior of smart glazing systems and their interactions with building thermal loads in a manner that reflects practical, rule-based operation rather than idealized or continuously optimized control.

Table 3. Thermal and optical properties for selected smart glazing products

Label	Manufacturer (Product)	U-factor (W/m²k)	SHGC (Clear-Dark)	VT (Clear-Dark)
SG1	Standard Dual Pane IGU (VIEW Inc)	1.65	0.46–0.09	0.58–0.03
SG2	SAGE (Classic TM Tempered)	1.59	0.47–0.09	0.62–0.02
SG3	Pleotint LLC (Clear + Suntuitive with Solarban [®] 60)	1.36	0.37–0.17	0.60–0.13
SG4	Double Glass Econtrol [®] Smart	1.10	0.42–0.10	0.56–0.10

2.4.1. Daylighting analysis

A daylighting analysis is carried out to quantify the interactions between visible transmittance and electric lighting demands. Specifically, daylight-responsive lighting controls are applied to all perimeter zones, each equipped with two photosensors positioned at a standard working-plane of 0.75 m (2.5 ft) high. These photosensors modulate electric lighting output to maintain an illuminance setpoint of 377 lux, consistent with the DOE prototype assumptions [36]. Continuous dimming is enabled with minimum lighting power and minimum light output fractions set to 0.2

[40]. This configuration allowed the analysis to isolate the contribution of smart glazing to lighting energy savings under both controlled and uncontrolled daylight conditions.

2.4.2. Parametric analysis

To explore the design space for smart glazing beyond commercially available products, a comprehensive parametric analysis is conducted by varying the SHGC from 0.0 to 0.9 in increments of 0.1. Corresponding visible transmittance values are derived using established relationships between SHGC and VT for smart glazing systems, with clear-state VT defined as $VT_H = 1.10 \times SHGC_H$ and dark-state VT as $VT_L = 1.10 \times SHGC_L$ [22]. The VT–SHGC relationship is a parametric design assumption rather than a product-specific representation. The U-factor is held constant, typically at $1.65 \text{ W/m}^2\cdot\text{K}$ but other values are considered as part of a sensitivity analysis, to isolate the influence of optical properties. For each combination of parameters, annual source energy use is estimated and compared against the baseline adiabatic window case (U-factor = SHGC = VT = AL = 0). Relative source energy change is used as the primary performance metric: negative values indicate that the smart glazed windows increase energy consumption representing a net energy liability, while positive values indicate net-positive energy performance for the smart glazed fenestration systems.

2.4.3. Sensitivity analysis

To identify and evaluate the contextual factors that drive the energy performance of smart glazed windows, additional sensitivity analyses are conducted. The U-factor of the smart glazed fenestration systems is varied to encompass three levels (0.5, 1.10, and $2.0 \text{ W/m}^2\cdot\text{K}$) to represent a spectrum from highly insulating to less efficient window types. Window-to-wall ratios of 15% and 45% are considered to capture the effects of façade design variations. The sensitivity analysis also considers different building sizes (small and large office prototypes) to reflect the effects of internal loads and footprint characteristics. Finally, a set of sensitivity analyses is performed across four representative U.S. climate locations: cool-dry climate of Boulder, CO (5B), cool-humid condition of Chicago, IL, mild climate of San Francisco, CA (3C), and hot climate of Phoenix, AZ (2B) [41].

3. Discussion of results

This section synthesizes the parametric and sensitivity analyses to systematically evaluate how switching control strategies, glazing optical and thermal properties, climate, geometry (WWR and building size), and U-factor collectively influence the net-positive energy potential of smart glazing systems when deployed in office buildings. The analysis provides application-oriented insights for commercially available products, identifying climate- and design-specific conditions under which smart glazing achieves substantial energy savings or, conversely, leads to energy penalties. In this study, a window system is considered net-positive if it reduces total annual building energy use, net-neutral if the total annual energy use of the building is equal to the reference baseline, and an energy liability if it increases total annual energy consumption, all relative to a baseline adiabatic window.

3.1. Influence of control strategies

The evaluation of the energy performance of smart glazed windows under different switching control strategies reveals that the choice of control variables substantially affects whole-building energy benefits for smart fenestration systems. OAT and ITSR are examined given their established relevance to solar heat gain dynamics and perimeter-zone thermal loads [26]. OAT, measured in °C, is a critical factor for heating and cooling thermal loads. ITSR, expressed in W/m², represents the total incident solar radiation, including beam, diffuse, and ground-reflected components [42]. Four commercially available smart glazing systems are evaluated in this section as outlined in [Table 3](#).

3.1.1 OAT-based switch controls

For the Boulder, CO prototype, the simulation results show that OAT-based switching controls consistently outperforms ITSR-based strategies. As illustrated in Fig. 4 (A), the highest energy savings are achieved at an OAT of 12 °C when daylighting control is active and 8 °C without daylighting control. The shift toward higher OAT values under daylighting control reflects the trade-off between the decrease in artificial lighting usage and the reduction in passive winter solar heat gains. Fig. 4 (B) illustrates that daylighting control reduces both cooling and lighting end energy uses but introduces a slight heating penalty when Standard Dual-Pane IGU (SG1) windows are employed. At moderate OAT settings, the reduction in cooling requirements and fan energy more than offsets the incremental heating demands.

Extending the analysis across multiple U.S. climates further highlights the climate dependency of optimal OAT settings (Figs. 5 and 6). In Chicago, IL, the optimal OAT is approximately 10 °C, both with and without daylighting control. In San Francisco, CA, the smart glazing systems achieve the lowest annual energy use at 12 °C with daylighting control and 10 °C without. For Phoenix, AZ, where cooling dominates the energy needs, the optimal OAT is near 6 °C, delaying the transition to high-transmittance states to limit unwanted solar gains throughout the year. The contrast between optimal OAT settings for heating-dominated climate of Chicago, IL, and cooling-dominated climate of Phoenix, AZ, outlined in Fig. 6 demonstrates that importance of switching the smart glazed fenestration systems to balance between heating, cooling, and lighting energy end used for each climate.

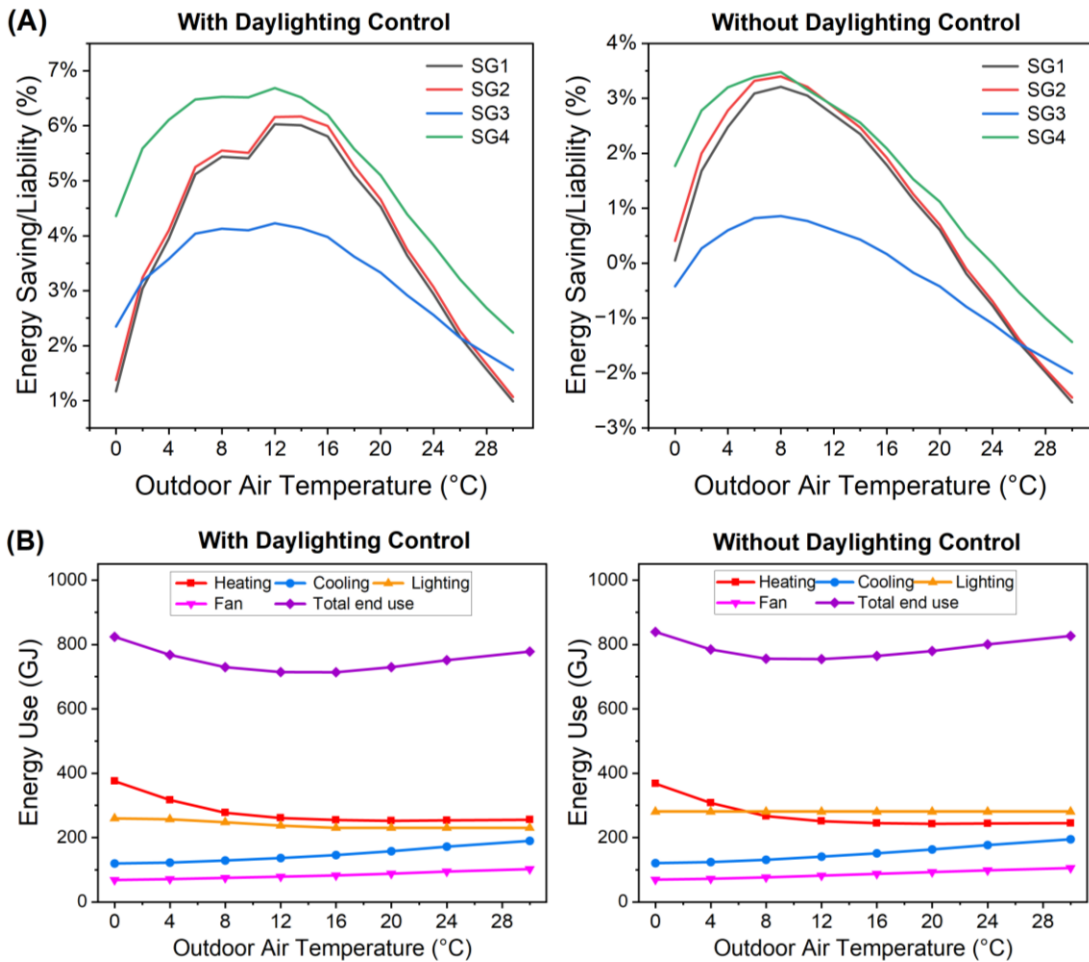


Fig. 4. OAT-based control performance for the Boulder, CO office building: (A) Annual energy savings for four smart glazing types, and (B) Breakdown of energy end uses for Standard Dual-Pane IGU (SG1) glazing, with and without daylighting control.

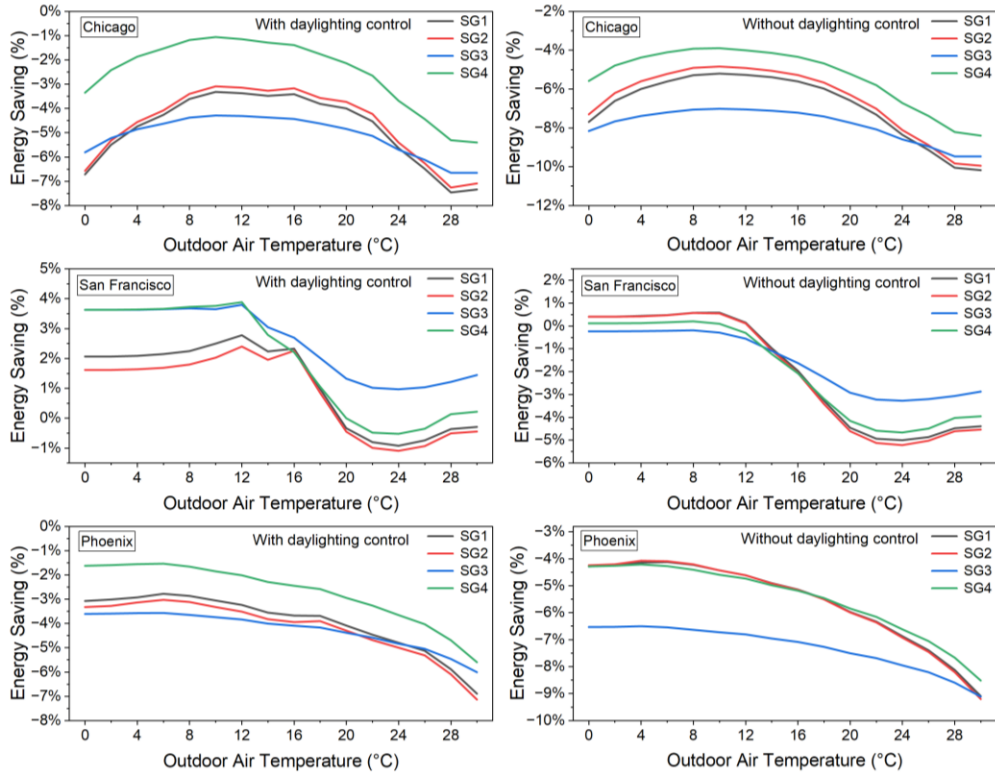


Fig. 5. Comparison of annual source energy savings for a medium office building across three U.S. climate zones using four smart glazing systems operated under OAT-based control, with and without daylighting control.

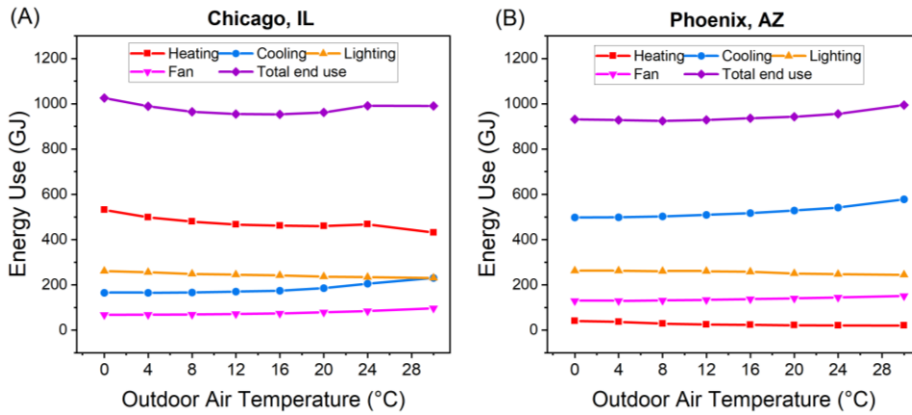


Fig. 6. Impact of outdoor temperatures on energy end use performance for office building with Standard Dual Pane IGU glazing (SG1) in (A) Chicago and (B) Phoenix, with daylighting control.

3.1.2 ITSR-based switch controls

ITSR-based switching controls provide lower energy benefits compared to OAT-based strategies. For Boulder, CO, the optimal ITSR threshold is approximately 350 W/m^2 , which mitigates

excessive solar heat gains while maintaining adequate daylight penetration (Fig. 7). Higher ITSR thresholds increase cooling loads due to unnecessary solar gains, whereas excessively low thresholds prematurely reduce glazing transmittance, increasing artificial lighting requirements. The climate dependency of ITSR-based control mirrors that of OAT-based strategies as can be seen in Fig. 8. For Chicago, IL, an optimal ITSR of 350 W/m² balances solar gains to reduce heating loads while limiting cooling energy use. Conversely, when the office building is in Phoenix, AZ, the optimal ITSR is near 0 W/m², reflecting the need to almost entirely eliminate any solar gains to minimize annual energy use. For this cooling-dominated climate, the limited benefits of additional daylight do not offset the increased cooling energy, demonstrating the importance of climate-specific ITSR thresholds. Across all climates, ITSR-based controls consistently underperform OAT-based controls, especially when daylighting control is deployed.

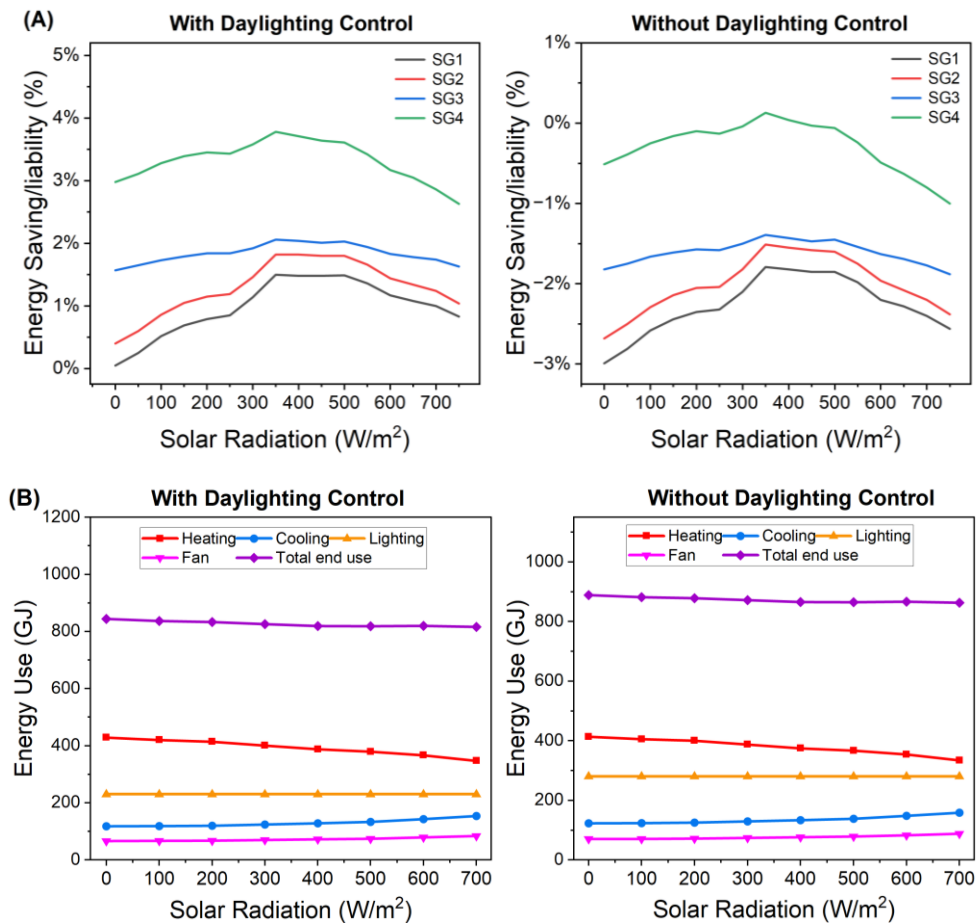


Fig. 7. ITSR-based control performance for the Boulder, CO, office building: (A) Annual energy savings for four smart glazing types, and (B) Breakdown of energy end uses for Standard Dual-Pane IGU (SG1) glazing, with and without daylighting control.

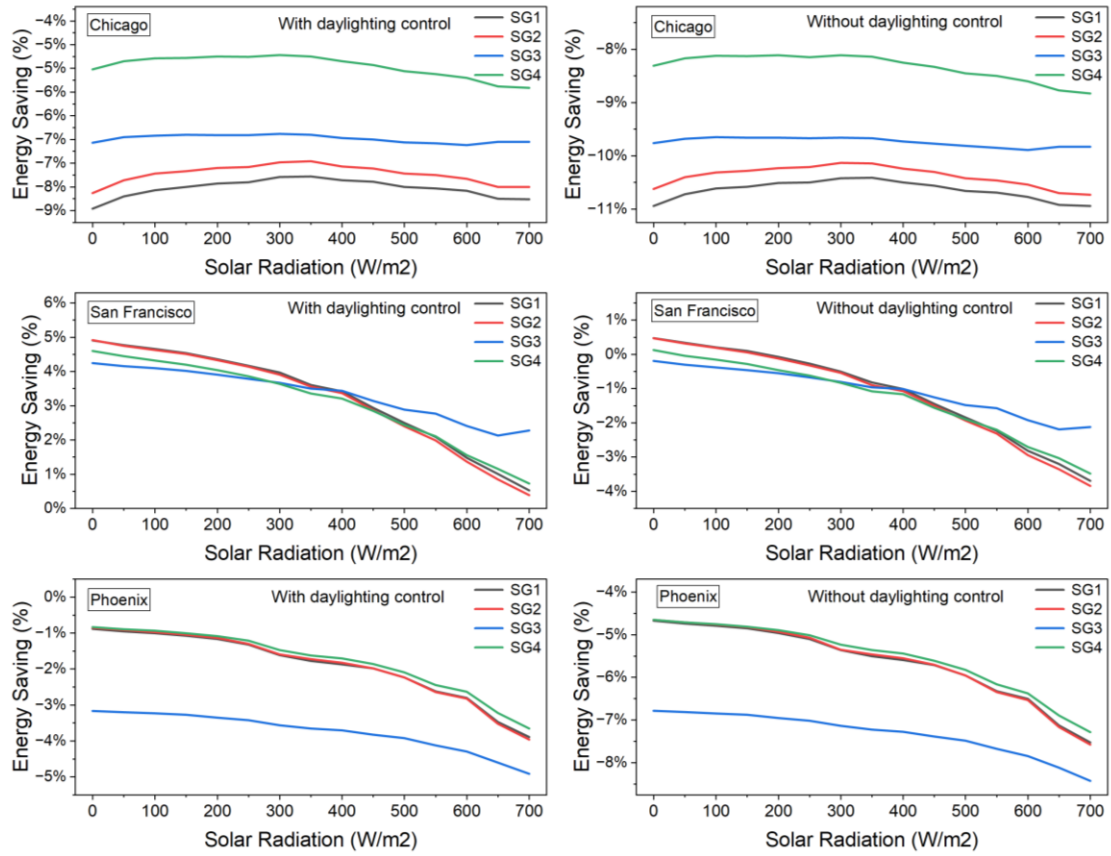


Fig. 8. Annual energy performance of medium office building in three US other climates for four smart glazing types using ITSR-based controls with and without daylighting control.

3.1.3 Comparative insights across climates

Comparing OAT- and ITSR-based strategies across four U.S. climates (Boulder, CO; Chicago, IL; San Francisco, CA; Phoenix, AZ) reveals that the optimal performance of smart glazing systems is strongly climate-dependent. OAT-based controls consistently outperform ITSR-based strategies across U.S. climates, with optimal setpoints varying by location and influenced by daylighting control, which reduces lighting and cooling needs but slightly increases heating demand. Table 4 summarizes the optimal OAT and ITSR thresholds and the associated energy savings for all evaluated climates. From a practical perspective, these findings suggest that OAT-based switching controls are more effective than ITSR-based strategies for achieving energy savings when applied to smart glazing systems, but their implementation requires careful consideration in real-world building automation systems. OAT-based switching is more feasible in real buildings, as temperature sensors are widely available and easily integrated into HVAC or building management

systems, whereas ITSR-based control is more complex and sensitive to sensor placement and maintenance requirement.

Table 4. Optimal switching settings of OAT and ITSR based controls for four US climates.

Climate	OAT Optimal control (°C)/ Percent savings		ITSR Optimal control (W/m ²) / Percent savings	
	With daylighting control	Without daylighting control	With daylighting control	Without daylighting control
Boulder, CO	12 °C / (6.7%)	8 °C / (3.5%)	350 W/m ² / (3.8%)	350 W/m ² / (0.13%)
Chicago, IL	10 °C / (-1%)	10 °C / (-4%)	350 W/m ² / (-5.3%)	350 W/m ² / (-8.1%)
San Francisco, CA	12 °C / (3.4%)	10 °C / (0.6%)	0 W/m ² / (4.9%)	0 W/m ² / (0.5%)
Phoenix, AZ	6 °C / (-1.5%)	6 °C / (-4%)	0 W/m ² / (-0.8%)	0 W/m ² / (-4.7%)

3.2. Effects of glazing optical properties

This section evaluates the impact of clear-state and dark-state SHGC characteristics on the energy behavior of an office building with smart glazing. Visible transmittance is assumed to scale proportionally with SHGC (i.e., $VT = 1.10 \cdot SHGC$ for all tint states) [[34], [41]], while the glazing U-factor is fixed at 1.65 W/m²·K. The analysis is performed using the optimal switching strategies for Boulder, CO (Table 4): OAT-based control at 12 °C with daylighting control and 8 °C without, and ITSR-based control at 350 W/m². Fig. 9 presents contour plots of annual energy change relative to the adiabatic baseline across all combinations of clear-state and dark-state SHGC values, with the diagonal indicating static glazing configurations.

Results show that many SHGC combinations achieve net energy savings at U-factor of 1.65 W/m²·K, and that daylighting control substantially expands the region of net-positive performance. Under OAT-based control with daylighting, annual energy use is reduced by up to 8% when clear-state SHGC exceeds 0.5 and dark-state SHGC remains below 0.1. Without daylighting control, achievable savings are more limited and peak at 5%, reflecting the importance of natural lighting in the energy performance contribution of smart glazed windows.

Fig. 10 shows that ITSR-based control at 350 W/m² performs significantly worse than OAT-based control. Energy savings are limited to 2% with daylighting control and shift to energy penalties (up to -1%) without daylighting across all SHGC combinations. These results indicate that, for Boulder, CO, temperature-driven switching is more effective than solar-radiation-based control for optimizing smart glazing performance.

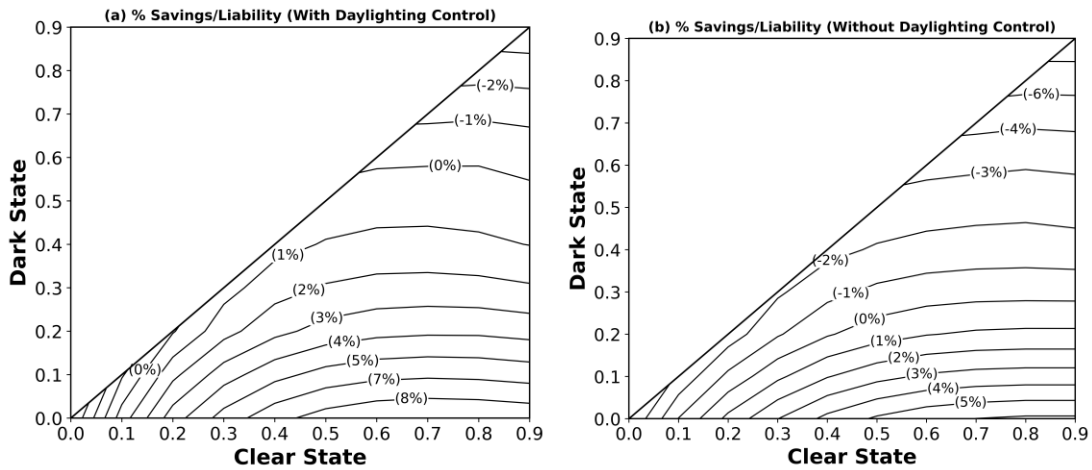


Fig. 9. Annual energy-saving contour plots for the Boulder, CO medium office prototype featuring smart glazing regulated by OAT-based switching: (a) with daylighting control and (b) without daylighting control.

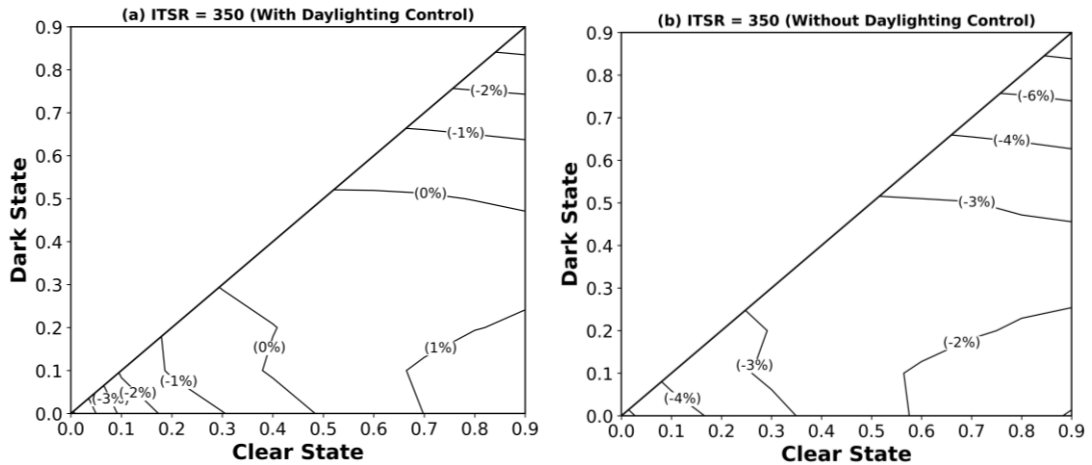


Fig. 10. Contour plots of annual energy performance for the Boulder, CO medium office prototype using smart glazing governed by ITSR-based switching: (a) with daylighting control and (b) without daylighting control.

3.3. Sensitivity analysis

3.3.1. Climate Dependence

This analysis evaluates how smart glazing optical properties affect the annual energy performance of a prototypical medium office building across three U.S. climate zones, assuming a constant U-factor of $1.65 \text{ W/m}^2\cdot\text{K}$ and the use of daylighting control. Fig. 11 presents contour maps showing

the influence of combined clear- and dark-state SHGC values on building energy use relative to the adiabatic baseline.

The results demonstrate a strong climate dependence, with net-neutral or net-positive performance achievable only within limited SHGC ranges. In Chicago, IL, most optical property combinations increase annual energy use, particularly when both glazing states permit high solar gains. Near-neutral performance is observed only within narrow design specifications where the clear-state SHGC ranges from approximately 0.7 to 0.9 and the dark-state SHGC is near 0.15, indicating limited tolerance for optical variation in cold climates.

For the mild climate of San Francisco, CA, a substantially wider range of SHGC combinations yields net energy benefits. With daylighting control, annual energy savings of up to approximately 4% are achieved when the clear-state SHGC lies between about 0.5 and 0.9 and the dark-state SHGC remains below 0.35.

For Phoenix, AZ, none of the evaluated SHGC combinations result in net-positive energy performance. Energy penalties exceeding (-20%) are observed due to dominant cooling loads and low OAT switching thresholds that keep the glazing in its dark state during most of the year. While this limits solar heat gains, it severely reduces daylight availability, increasing lighting and heating demands enough to outweigh cooling savings.

Overall, these findings highlight the necessity of climate-specific selection of smart glazing optical properties and control strategies. Even with daylighting control, inappropriate SHGC combinations can result in substantial energy penalties, emphasizing the importance of integrated, climate-responsive design for smart glazed office buildings.

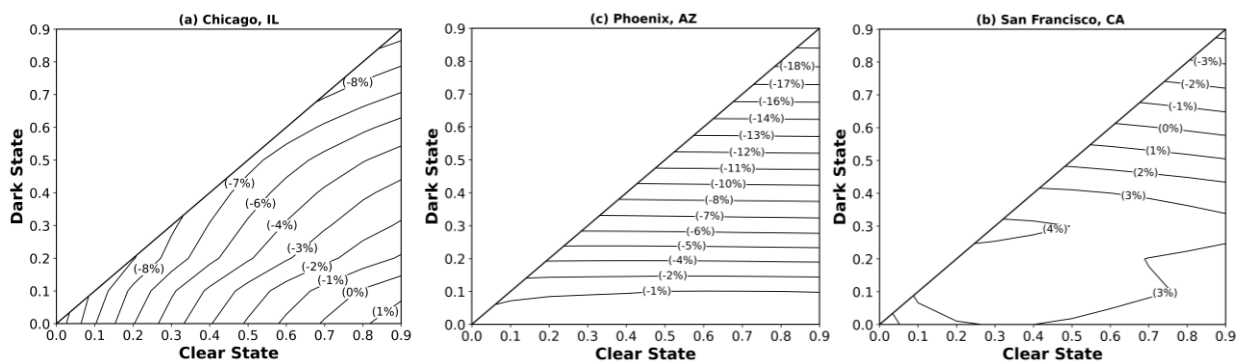


Fig. 11. Contour plots showing annual energy savings or penalties of smart glazing systems with different optical properties for the medium office building in three U.S. climate zones: (a) Chicago, IL (b) San Francisco, CA, and (c) Phoenix, AZ.

3.3.2. Impact of window-to-wall ratio

A parametric analysis is performed to assess the impact of WWR on the energy performance of the medium-sized office building in Boulder, CO. In this section, two façade configurations are considered, representing relatively small (15%) and large (45%) window areas with daylighting control. The results shown in Fig. 14 highlight a notable change in how smart glazing and its optical properties influence the overall energy consumption of office building as the WWR increases. At a WWR of 15%, smart glazing has only a modest effect on annual energy use. Across the full range of clear- and dark-state SHGC values, variations in source energy remain limited, suggesting that when window areas are small, differences in solar heat gains and daylight between clear and dark states have only a minor impact on total building energy demand.

The impact of smart glazing on energy use becomes significantly more pronounced at a WWR of 45%. With larger window areas, the building's energy demand is highly sensitive to the optical properties of the smart glazing. Depending on the combination of clear- and dark-state SHGC values, energy performance can range from modest savings to substantial increases, with penalties reaching up to 15% for certain configurations. This increased sensitivity highlights the amplified effect of solar gains and daylight contributions in buildings with extensive fenestration. Overall, the analysis indicates that the advantages and drawbacks of smart glazing are strongly dependent on window area. Buildings with small glazing fractions exhibit relatively stable energy performance regardless of switching strategies, whereas those with large glazing areas require careful selection of optical properties and control settings to prevent significant energy penalties.

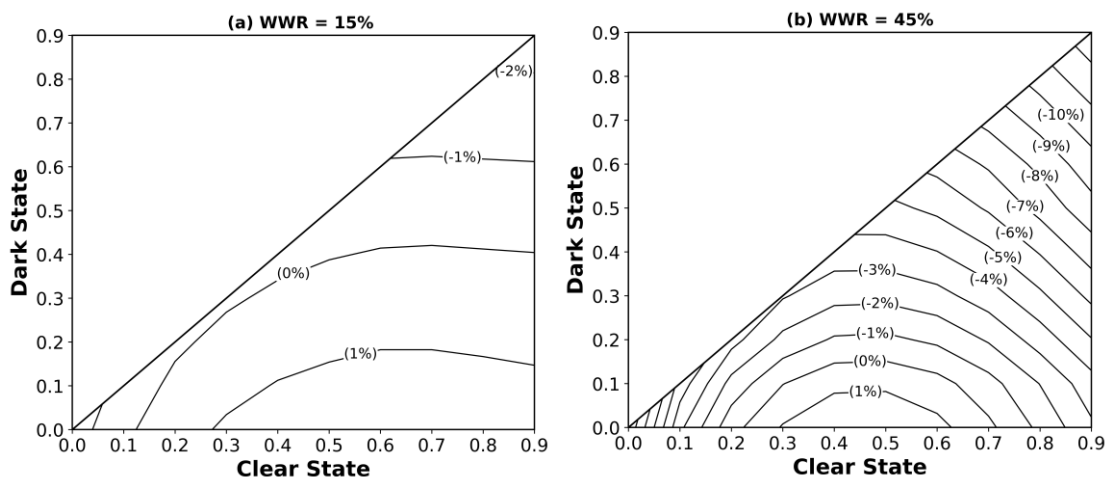


Fig. 12. Energy performance contours of smart glazing for a medium office building at WWRs of (a) 15% and (b) 45%, evaluated with and without daylighting control in Boulder, CO.

3.3.3. Impact of switch controls

The impact of different switching settings under OAT- and ITSR-based control strategies are assessed for the prototypical office building in Boulder, Colorado. Figures 13 and 14 illustrate how the optical properties of the smart glazing influence annual energy performance for two alternative OAT and ITSR setpoints, beyond the optimal values identified in Section 3.1. The results show that the choice of switching setting strongly influence the effectiveness of the smart glazed fenestration systems, and the interactions with daylighting control further affect substantially the energy performance of the office building. For the OAT-based control strategies, the contour plots illustrate that lower switching outdoor air temperatures generally yield higher energy savings. When the glazing transitions at $OAT=5^{\circ}C$, annual savings approach 8%. However, at $OAT=20^{\circ}C$, the maximum energy benefits are reduced to 5% annual reduction. The improved performance at $OAT=5^{\circ}C$ reflects the heating dominated nature of the climate of Boulder, CO, where harvesting solar heat gains during colder periods reduces winter heating demands.

However, the previously identified optimal $OAT=12^{\circ}C$ switching setting outperforms both $OAT=5^{\circ}C$ and $OAT=20^{\circ}C$. To achieve similar annual energy savings levels, using $OAT=12^{\circ}C$ as switching setting maintains a substantially broader feasible range of SHGC combinations. For example, an 8% level of annual energy savings is attainable across clear-state SHGC ranging from 0.45 to 0.90 and dark-state SHGC varying between 0 and 0.05. In contrast, the use of $OAT=5^{\circ}C$ setting achieves similar annual energy savings only within a much narrower range of optical properties concentrated at higher clear-state SHGC values. The comparison confirms that $OAT=12^{\circ}C$ offers the best overall balance between reducing heating demands and avoiding unnecessary cooling penalties. Fig. 14 presents the variation of office building energy performance with different ITSR switching settings using the ITSR-based controls. As the ITSR switching setting increases from 250 W/m^2 to 450 W/m^2 , the deployment of smart glazing windows progressively shifts from marginally helpful to consistently detrimental. At the highest ITSR setting, even when daylighting control is active, the smart glazed fenestration system becomes an energy liability, increasing annual energy use by roughly 1%–3%. This behavior is due to the fact that higher ITSR settings allow excessive solar heat gains resulting in higher cooling loads outweighing any reductions in lighting energy needs.

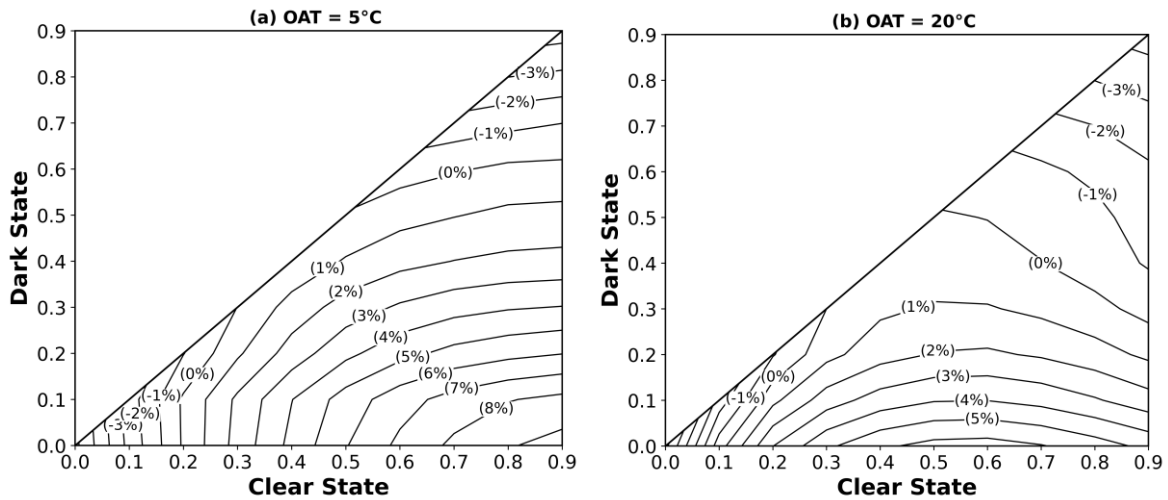


Fig. 13. Energy performance contours of smart glazing for a medium office building under OAT-based switching at (a) 5 °C and (b) 20 °C, evaluated with daylighting control in Boulder, CO.

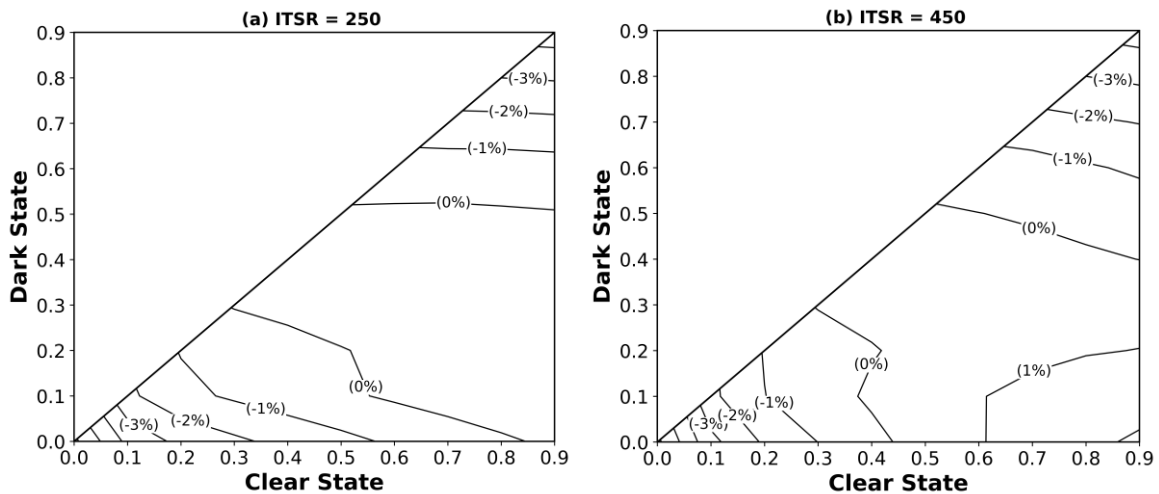


Fig. 14. Energy performance contours of smart glazing for a medium office building under ITSR-based switching at (a) 250 W/m² and (b) 450 W/m², with daylighting control in Boulder, CO.

3.3.4. Influence of Building Size

To evaluate the effect of building size on the performance of smart glazed fenestration systems, the analysis is extended to include small and large office buildings, each compared with its corresponding adiabatic baseline. The results presented in Fig. 15 show a clear dependence of the energy efficiency benefits of smart glazed windows on the building size using Boulder, CO,

climate. Among the three prototypes, the small office building demonstrates the greatest capacity to realize net-positive energy performance, particularly when daylighting control is implemented. For a wide range of clear- and dark-state SHGC combinations, the small office building achieves annual energy reductions exceeding 2% relative to its baseline. By comparison, the large office building reaches net-neutral energy performance only for limited optical properties for smart glazed windows. This result can be attributed to variations in thermal interactions between indoors and outdoors due to the differences in geometric characteristics. The small office building, with its higher surface-area-to-volume ratio, is more responsive to changes in solar heat gains, heat transmissions, and daylight intakes, allowing the smart glazed windows to have a stronger influence on heating, cooling, and lighting loads. The large office building, characterized by a much larger internal volume and lower relative exposure to the outdoors, exhibits reduced contribution of the glazed fenestration system on thermal loads and daylighting apertures. The analysis conducted in this section clearly suggests that the benefits of smart glazed windows and their abilities to achieve NPW performance are highly dependent on the building’s architectural and its geometric characteristics.

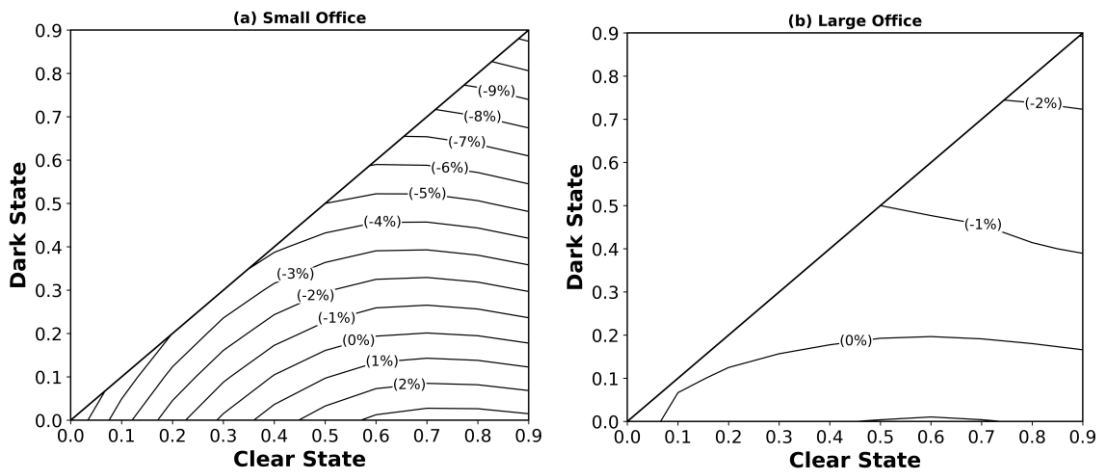


Fig. 15. Energy performance contours of smart glazing with daylighting control for (a) a small office building and (b) a large office building in Boulder, Colorado.

3.3.5. Impact of U-factor

Fig. 16 illustrates how variations in glazing U-factor influence yearly energy outcomes for a representative office building located in Boulder, Colorado, when operated with an OAT-based

switching strategy and daylighting control. Changes in window thermal transmittance noticeably affect both the magnitude of potential energy savings and the set of optical property combinations that result in net-positive energy performance. For glazing systems with a relatively high U-factor of $2.0 \text{ W/m}^2\cdot\text{K}$, the maximum decrease in yearly energy consumption is approximately 8% relative to the baseline condition. Reducing the U-factor to $1.10 \text{ W/m}^2\cdot\text{K}$ maintains a similar maximal level of annual energy savings but substantially broadens the set of clear- and dark-state SHGC combinations that allow net-positive energy performance for the smart glazed windows. Additional enhancements in thermal performance, reflected by a U-factor of $0.50 \text{ W/m}^2\cdot\text{K}$, do not lead to higher peak energy savings. Instead, the feasible range of optical properties that support net-positive energy performance becomes more limited. The findings indicate diminishing marginal gains as the thermal transmittance of smart glazing is reduced. A U-factor of approximately $1.10 \text{ W/m}^2\cdot\text{K}$ is adequate to support a broad spectrum of optical configurations that achieve net-positive window performance, while further reductions in U-factor provide little additional improvement in overall energy outcomes.

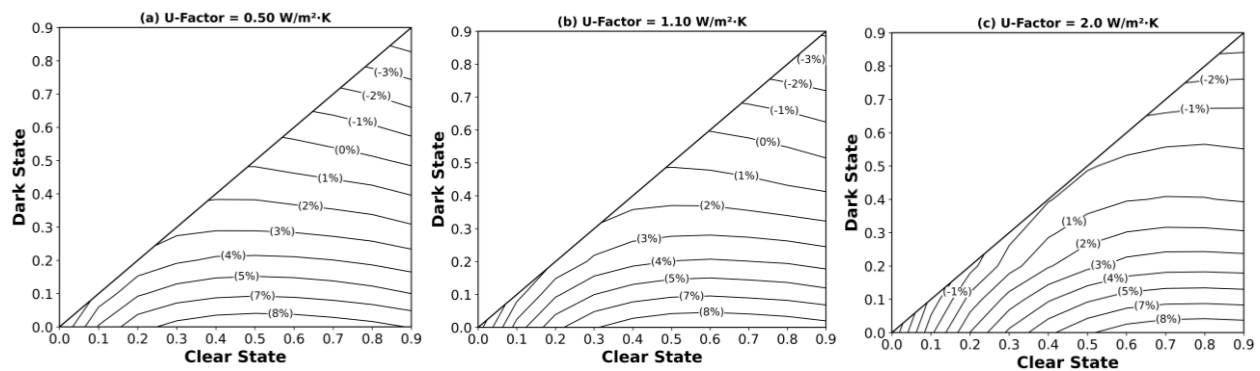


Fig. 16. Energy performance contours of smart glazing with U-factors of (a) $0.50 \text{ W/m}^2\cdot\text{K}$, (b) $1.10 \text{ W/m}^2\cdot\text{K}$, and (c) $2.00 \text{ W/m}^2\cdot\text{K}$ for a representative office building case, evaluated in Boulder, CO.

3.3 Applications

This section builds on the optimization and parametric analyses presented in Sections 3.1 and 3.2 to evaluate whether commercially available smart glazing systems can achieve net-positive window (NPW) performance for office buildings under a range of design and operational scenarios. Four commercially available smart glazing products, selected from Table 1, are

examined to assess their NPW potential when applied to medium office buildings across different U.S. climate zones. The glazing systems considered include:

- Glazing 1: SAGEGLASS GREEN, U-factor = $1.65 \text{ W/m}^2\cdot\text{K}$, SHGC clear/dark = 0.27/0.10, VT clear/dark = 0.49/0.01
- Glazing 2: SAGEGLASS GRAY, U-factor = $1.65 \text{ W/m}^2\cdot\text{K}$, SHGC clear/dark = 0.33/0.10, VT clear/dark = 0.45/0.01
- Glazing 3: Dual IGU Blue Tint, U-factor = $1.65 \text{ W/m}^2\cdot\text{K}$, SHGC clear/dark = 0.43/0.09, VT clear/dark = 0.36/0.02
- Glazing 4: Standard Dual Pane IGU, U-factor = $1.65 \text{ W/m}^2\cdot\text{K}$, SHGC clear/dark = 0.43/0.09, VT clear/dark = 0.36/0.02

3.3.1. Assessments of smart glazings in four US climate zones

Fig. 17 presents a climate-sensitivity assessment of four commercially available smart glazing systems evaluated at a fixed U-factor of $1.65 \text{ W/m}^2\cdot\text{K}$. The results reveal a pronounced influence of climate on smart glazing energy outcomes. In Boulder, CO, and San Francisco, AZ, all four glazing products achieve net-positive energy performance, whereas in Chicago, IL, and Phoenix, AZ, the same systems lead to higher annual energy use compared to the adiabatic window used as a reference case. For the Boulder case, the annual reduction in energy use spans from approximately 3.5% for Glazing 1 to about 6.5% for Glazing 4. The same glazing types deployed in San Francisco, produce comparable annual energy savings. In contrast, deployment of any glazing type for an office building in Chicago, IL, results in increased annual energy consumption. The magnitude of the energy penalties varies by the glazing type, with increases of roughly 6.5%, 6%, 3.5%, and 3% for Glazing 1 through Glazing 4. A similar pattern is observed in Phoenix, AZ, as all the four glazing types increase annual energy use by about 2% relative to the baseline. These findings demonstrate that the performance of smart glazed windows is highly climate-specific. Glazing systems that deliver clear energy benefits in temperate or heating-leaning climates may become energy liabilities in cold or cooling-dominated regions. Therefore, a detailed climate-appropriate analysis is essential before specifying any smart glazing technologies for office buildings, combined with careful consideration of switching settings and associated control strategies.

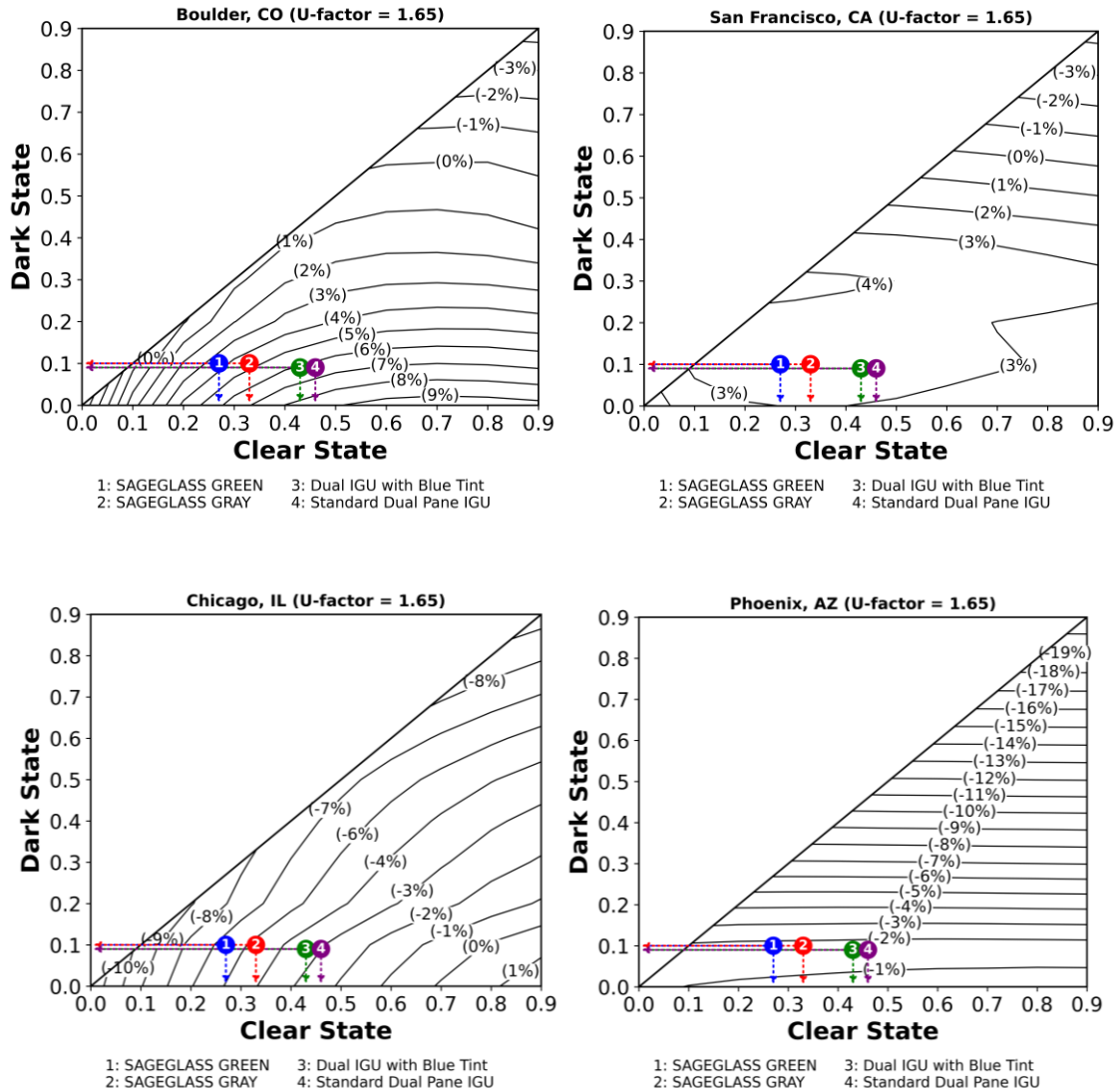


Fig. 17. Assessment of net-positive window performance for four commercially available smart glazing systems across office buildings in four representative U.S. climate zones.

3.3.2. Assessments of smart glazed windows based on their size

The effect of window size on the net-positive energy performance of smart glazing systems was assessed for an office building in Boulder, CO, considering WWR of 15% and 45%. As illustrated in Fig. 18, all four glazing types achieve net-positive energy operation when applied to the smaller façade configuration (i.e., WWR = 15%), with annual energy savings ranging between 0.5% and 1.2% relative to the adiabatic baseline. However, when the glazing area increases to WWR=45%, the windows energy performance diverges significantly across the glazing types. Only Glazing 3

and Glazing 4 maintain net positive energy performance, each reducing annual energy use by about 1%, whereas Glazing 1 results in increased energy consumption comparative to glazing size of WWR=15%. The reduced effectiveness at higher WWR stems from the fact that solar gains and conductive losses/gains through the glazing play a more dominant role for large than small window case. The results emphasize that the ability of smart glazing to achieve net positive energy status is strongly dependent on the window size. High glazed buildings require smart glazed windows with optimized optical properties to avoid energy penalties.

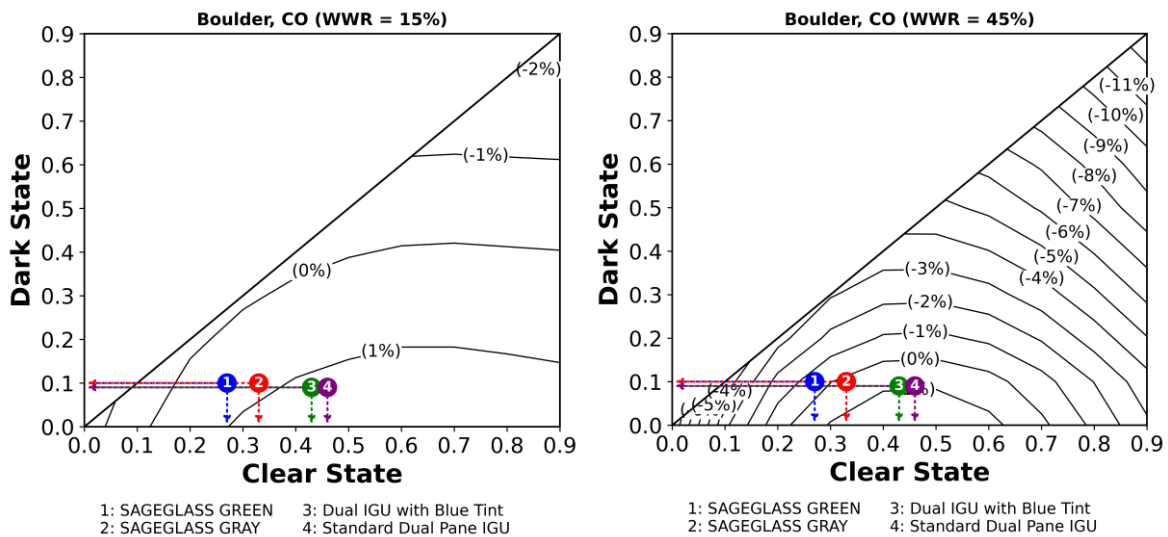


Fig. 18. Evaluation of net-positive energy performance for four smart glazing systems at WWR of 15% and 45% in office buildings located in Boulder, CO.

3.3.3. Assessments of smart glazing using different switching controls

The effects of optimizing switching controls for smart glazing systems are examined for a representative office building in Boulder, Colorado. Fig. 19 shows how adjustments to the OAT setpoint affect the building’s annual energy outcomes for each of the four glazing types. A lower switching temperature consistently increases energy savings, with all glazing systems performing better when the OAT setpoint is reduced from 20 °C to 5 °C. For example, the Dual IGU with Blue Tint (Glazing 3) and the Standard Dual Pane IGU (Glazing 4) achieve annual energy savings of roughly 5% at OAT=5°C, compared with about 4% at OAT=20°C. In contrast, the SAGEGLASS Green (Glazing 1) and Gray (Glazing 2) products show only marginal differences in energy performance between the two OAT settings. The outcomes indicate that the switching temperature

plays a significant role in determining the effectiveness of smart glazed windows, although the degree of sensitivity varies by the glazing type. Selecting an appropriate OAT switching setting together with the glazing's optical characteristics is therefore essential when configuring smart window systems to maximize energy performance for office buildings.

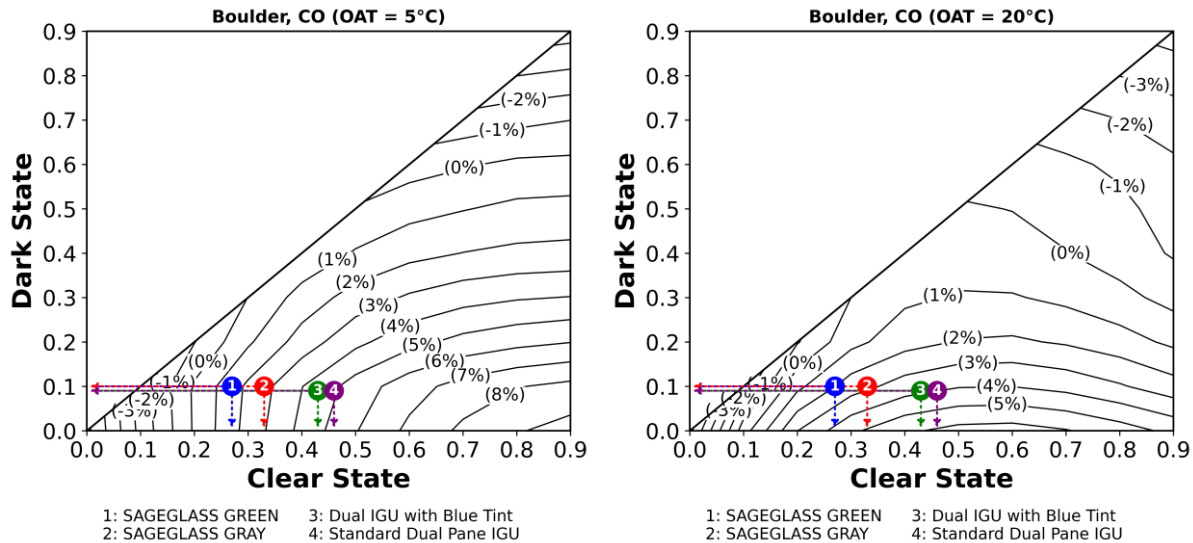


Fig. 19. Evaluation of net-positive energy performance for four smart glazing systems at two OAT-based switching setpoints in office buildings located in Boulder, CO.

4. Summary and Conclusions

This study evaluated the feasibility of achieving net-positive window (NPW) performance using smart glazing systems in office buildings through a comprehensive parametric analysis. The results demonstrate that NPW performance is influenced by a combination of factors, including optical and thermal properties of the glazing, switching control strategies, local climate, window-to-wall ratio (WWR), building geometry, and integration with daylighting systems. Key findings from the analysis include:

- OAT-based switching consistently outperforms ITSR-based control across climates, building sizes, and window-to-wall ratios.
- Smart glazing rarely achieves net positive energy performance without dimmable daylighting integration.

- Heating-dominated and mild climates support net positive window operation, while cooling-dominated climates can impose energy penalties up to 20% if controls and optical properties are not optimized.
- Clear-state SHGC of 0.45–0.65 and dark-state SHGC of 0.10–0.25, across U-factors of 0.50–2.00 W/m²·K, enable NPW performance, whereas reducing U-factor below 1.10 W/m²·K offers limited additional benefits.
- Smaller buildings with moderate WWR ($\leq 33\%$) allow for wider variations in glazing properties, while larger buildings with higher WWR require more specific design specifications.

In conclusion, smart glazed fenestration systems can achieve NPW performance in office buildings when carefully designed and operated. To maximize energy benefits of smart glazed windows:

1. Select OAT-based switching controls for practical and robust performance.
2. Optimize clear and dark-state SHGC and visible transmittance values to match building size, geometry, and local climate.
3. Integrate dimmable daylighting control to capture both thermal and lighting energy savings.
4. Consider building geometry, internal loads, and WWR holistically to ensure NPW feasibility.
5. Prioritize optical switching behavior over ultra-low U-factors, as the latter has limited impact beyond 1.10 W/m²·K for office buildings.

The findings outlined in this study can provide manufacturers, designers, and policymakers with clear guidelines for the required specifications for smart glazed fenestration systems to maximize their energy performance when deployed for office buildings. While NPW performance, as evaluated in this study, is an energy-based metric and does not capture visual comfort, glare, or view quality, the findings provide a systematic quantitative foundation for estimating the net energy contribution of smart glazing systems. These results offer clear guidance for manufacturers, designers, and policymakers seeking to maximize the energy performance of smart glazed fenestration systems and support the transition toward net-zero and net-positive commercial buildings.

Acknowledgement

This research was funded by the Building Energy Smart Technologies (BEST) Center, established by National Science Foundation (NSF) under grant numbers 2113874 and 2113907.

Disclosure

MDM is a cofounder of Tynt Technologies.

References

- [1] C. Robinson *et al.*, “Machine learning approaches for estimating commercial building energy consumption,” *Appl. Energy*, vol. 208, pp. 889–904, Dec. 2017, doi: 10.1016/j.apenergy.2017.09.060.
- [2] M. Krarti, P. M. Erickson, and T. C. Hillman, “A simplified method to estimate energy savings of artificial lighting use from daylighting,” *Build. Environ.*, vol. 40, no. 6, pp. 747–754, Jun. 2005, doi: 10.1016/j.buildenv.2004.08.007.
- [3] P. C. H. Yu and W. K. Chow, “Energy use in commercial buildings in Hong Kong,” *Appl. Energy*, vol. 69, no. 4, pp. 243–255, Aug. 2001, doi: 10.1016/S0306-2619(01)00011-3.
- [4] Y. Huang, J. Niu, and T. Chung, “Study on performance of energy-efficient retrofitting measures on commercial building external walls in cooling-dominant cities,” *Appl. Energy*, vol. 103, pp. 97–108, Mar. 2013, doi: 10.1016/j.apenergy.2012.09.003.
- [5] A. Charles, W. Maref, and C. M. Ouellet-Plamondon, “Case study of the upgrade of an existing office building for low energy consumption and low carbon emissions,” *Energy Build.*, vol. 183, pp. 151–160, Jan. 2019, doi: 10.1016/j.enbuild.2018.10.008.
- [6] A. Gustavsen, B. P. Jelle, D. Arasteh, and C. Kohler, “State-of-the-Art Highly Insulating Window Frames - Research and Market Review,” Lawrence Berkeley National Laboratory (LBNL), Berkeley, CA, Jan. 2007. doi: 10.2172/941673.
- [7] M. Casini, “Active dynamic windows for buildings: A review,” *Renew. Energy*, vol. 119, pp. 923–934, Apr. 2018, doi: 10.1016/j.renene.2017.12.049.
- [8] C. Harris, “Pathway to Zero Energy Windows: Advancing Technologies and Market Adoption,” National Renewable Energy Laboratory (NREL), Golden, CO (United States), Apr. 2022. doi: 10.2172/1866581.
- [9] D. L. Villa, N. T. Hahn, J. K. Grey, and F. Pavich, “Futures for electrochromic windows on high performance houses in arid, cold climates,” *Energy Build.*, vol. 315, p. 114293, Jul. 2024, doi: 10.1016/j.enbuild.2024.114293.
- [10] V. Costanzo, G. Evola, and L. Marletta, “Thermal and visual performance of real and theoretical thermochromic glazing solutions for office buildings,” *Sol. Energy Mater. Sol. Cells*, vol. 149, pp. 110–120, May 2016, doi: 10.1016/j.solmat.2016.01.008.
- [11] X. Zhao, A. Aili, D. Zhao, D. Xu, X. Yin, and R. Yang, “Dynamic glazing with switchable solar reflectance for radiative cooling and solar heating,” *Cell Rep. Phys. Sci.*, vol. 3, no. 4, p. 100853, Apr. 2022, doi: 10.1016/j.xcrp.2022.100853.

- [12] M. Detsi, I. Atsonios, I. Mandilaras, and M. Founti, “Effect of smart glazing with electrochromic and thermochromic layers on building’s energy efficiency and cost,” *Energy Build.*, vol. 319, p. 114553, Sep. 2024, doi: 10.1016/j.enbuild.2024.114553.
- [13] N. L. Sbar, L. Podbelski, H. M. Yang, and B. Pease, “Electrochromic dynamic windows for office buildings,” *Int. J. Sustain. Built Environ.*, vol. 1, no. 1, pp. 125–139, Jun. 2012, doi: 10.1016/j.ijbsbe.2012.09.001.
- [14] M. Riganti, G. Li Castri, V. Serra, M. Manca, and F. Favoino, “Energy saving potential of advanced dual-band electrochromic smart windows for office integration,” *Energy Build.*, vol. 327, p. 115084, Jan. 2025, doi: 10.1016/j.enbuild.2024.115084.
- [15] D. Arasteh, H. Goudey, J. Huang, C. Kohler, and R. Mitchell, “Performance Criteria for Residential Zero Energy Windows,” 2006.
- [16] Selkowitz, S; Hart, R; Curcija, C, “Breaking the 20 Year Logjam to Better Insulating Windows,” 2018, doi: 10.20357/B76K5K.
- [17] H. Gundogdu, M. Terkes, A. Demirci, and U. Cali, “Assessing energy savings and visual comfort with PDLC-based smart window in an Istanbul office building: A case study,” *Energy Rep.*, vol. 12, pp. 4252–4265, Dec. 2024, doi: 10.1016/j.egyr.2024.10.009.
- [18] Grand View Research, “Smart Glass Market Summary.” Accessed: Aug. 15, 2025. [Online]. Available: <https://www.grandviewresearch.com/industry-analysis/smart-glass-market#>
- [19] M. Roostaei Firouzabad and F. Razi Astaraei, “Energetical effect of electrochromic glazing on the double-skin façade of the building in different climates,” *Energy Build.*, vol. 316, p. 114344, Aug. 2024, doi: 10.1016/j.enbuild.2024.114344.
- [20] J. Y. Zheng *et al.*, “Review on recent progress in WO₃-based electrochromic films: preparation methods and performance enhancement strategies,” *Nanoscale*, vol. 15, no. 1, pp. 63–79, 2023, doi: 10.1039/d2nr04761f.
- [21] M. N. Mustafa, M. A. A. Mohd Abdah, A. Numan, A. Moreno-Rangel, A. Radwan, and M. Khalid, “Smart window technology and its potential for net-zero buildings: A review,” *Renew. Sustain. Energy Rev.*, vol. 181, p. 113355, Jul. 2023, doi: 10.1016/j.rser.2023.113355.
- [22] M. Krarti, “Energy performance of control strategies for smart glazed windows applied to office buildings,” *J. Build. Eng.*, vol. 45, p. 103462, Jan. 2022, doi: 10.1016/j.jobeb.2021.103462.
- [23] A. Jonsson and A. Roos, “Evaluation of control strategies for different smart window combinations using computer simulations,” *Sol. Energy*, vol. 84, no. 1, pp. 1–9, Jan. 2010, doi: 10.1016/j.solener.2009.10.021.
- [24] A. Aldawoud, “Conventional fixed shading devices in comparison to an electrochromic glazing system in hot, dry climate,” *Energy Build.*, vol. 59, pp. 104–110, Apr. 2013, doi: 10.1016/j.enbuild.2012.12.031.
- [25] P. Tavares, H. Bernardo, A. Gaspar, and A. Martins, “Control criteria of electrochromic glasses for energy savings in mediterranean buildings refurbishment,” *Sol. Energy*, vol. 134, pp. 236–250, Sep. 2016, doi: 10.1016/j.solener.2016.04.022.
- [26] N. A. Lantonio and M. Krarti, “Simultaneous design and control optimization of smart glazed windows,” *Appl. Energy*, vol. 328, p. 120239, Dec. 2022, doi: 10.1016/j.apenergy.2022.120239.
- [27] P. Tavares, H. Bernardo, A. Gaspar, and A. Martins, “Control criteria of electrochromic glasses for energy savings in mediterranean buildings refurbishment,” *Sol. Energy*, vol. 134, pp. 236–250, Sep. 2016, doi: 10.1016/j.solener.2016.04.022.

- [28] A. Aldawoud, “Conventional fixed shading devices in comparison to an electrochromic glazing system in hot, dry climate,” *Energy Build.*, vol. 59, pp. 104–110, Apr. 2013, doi: 10.1016/j.enbuild.2012.12.031.
- [29] L. L. Fernandes, E. S. Lee, and G. Ward, “Lighting energy savings potential of split-pane electrochromic windows controlled for daylighting with visual comfort,” *Energy Build.*, vol. 61, pp. 8–20, Jun. 2013, doi: 10.1016/j.enbuild.2012.10.057.
- [30] D. T. Gillaspie, R. C. Tenent, and A. C. Dillon, “Metal-oxide films for electrochromic applications: present technology and future directions,” *J. Mater. Chem.*, vol. 20, no. 43, p. 9585, 2010, doi: 10.1039/c0jm00604a.
- [31] R. Huang, Y. Xie, N. Cao, X. Jia, and D. Chao, “Self-powered electrochromic smart window helps net-zero energy buildings,” *Nano Energy*, vol. 129, p. 109989, Oct. 2024, doi: 10.1016/j.nanoen.2024.109989.
- [32] S. D. Rezaei, S. Shannigrahi, and S. Ramakrishna, “A review of conventional, advanced, and smart glazing technologies and materials for improving indoor environment,” *Sol. Energy Mater. Sol. Cells*, vol. 159, pp. 26–51, Jan. 2017, doi: 10.1016/j.solmat.2016.08.026.
- [33] J. Apte and D. Arasteh, “Future Advanced Windows for Zero-Energy Homes,” *ASHRAE Trans.*, vol. 109, no. 2, pp. 871–882, 2003.
- [34] E. Ohene, M. D. McGehee, and M. Krarti, “Quantifying energy benefits from window improvement strategies for commercial buildings,” *Energy Build.*, vol. 347, p. 116239, Nov. 2025, doi: 10.1016/j.enbuild.2025.116239.
- [35] R. Tällberg, B. P. Jelle, R. Loonen, T. Gao, and M. Hamdy, “Comparison of the energy saving potential of adaptive and controllable smart windows: A state-of-the-art review and simulation studies of thermochromic, photochromic and electrochromic technologies,” *Sol. Energy Mater. Sol. Cells*, vol. 200, p. 109828, Sep. 2019, doi: 10.1016/j.solmat.2019.02.041.
- [36] DOE and PNNL, “Commercial Prototype Building Models,” Pacific Northwest National Laboratory, Richland, WA, 2023. [Online]. Available: https://www.energycodes.gov/development/commercial/prototype_models
- [37] D. B. Crawley, L. K. Lawrie, C. O. Pedersen, and F. C. Winkelmann, “EnergyPlus: Energy Simulation Program,” *ASHRAE journal*, vol. 42, no. 4, pp. 49–56, 2000.
- [38] Department of Energy, “Commercial prototype building,” 2021. [Online]. Available: <https://www.energycodes.gov/prototype-building-models#Commercial>
- [39] P. Ihm, L. Park, M. Krarti, and D. Seo, “Impact of window selection on the energy performance of residential buildings in South Korea,” *Energy Policy*, vol. 44, pp. 1–9, May 2012, doi: 10.1016/j.enpol.2011.08.046.
- [40] EnergyPlus, “Engineering Manual, EnergyPlus.” Accessed: Jan. 08, 2025. [Online]. Available: <https://bigladdersoftware.com/epx/docs/8-0/input-output-reference/page-016.html>
- [41] M. Krarti, “Optimal optical properties for smart glazed windows applied to residential buildings,” *Energy*, vol. 278, p. 128017, Sep. 2023, doi: 10.1016/j.energy.2023.128017.
- [42] EnergyPlus, “Input Output Reference,” 2022, [Online]. Available: https://energyplus.net/assets/nrel_custom/pdfs/pdfs_v22.1.0/InputOutputReference.pdf